Oxidative Coupling of Phenols. Part 7.[1] Spin-density Calculations on the Phenoxyl Radical

David R. Armstrong, Colin Cameron, Derek C. Nonhebel, and Peter G. Perkins *
Department of Pure and Applied Chemistry, University of Strathclyde, Glasgow G1 1XL

The calculation of the spin-density distribution and other properties of the phenoxyl radical by a variety of *ab initio* MO techniques is described. The relative importance of basis-set size to structural factors was investigated and the results indicate that the geometry of the radical is a more important feature in arriving at a satisfactory theoretical description of the spin-density distribution in the phenoxyl radical than is the basis set.

There are suggestions in the literature [2,3] that the distribution of the unpaired electron in a phenoxyl radical is the overriding factor which determines the relative proportions of the various coupled products formed in the oxidative coupling of phenols, the most notable case being that of orcinol.[4] In the preceding paper [1] we have, however, shown that, in the oxidations of phenol and 3,5-dimethylphenol, the relative ratios of the C–C coupled dimers are not determined by the spin-density distribution in the phenoxyl radicals. The results obtained could, however, be satisfactorily interpreted if the radicals preferentially approach each other in a sandwich-like manner *via* the transition state (Figure 1). We shall consider the coupling process in detail in Part 8.[5] However, in this paper we focus attention on the spin-density distribution in the phenoxyl radical. This is necessary before it is possible to carry out a theoretical study on the preferred mode of coupling of phenoxyl radicals.

A number of calculations on the phenoxyl radical and related species have been reported, produced from a variety of quantum mechanical methods. Some of these have been more successful [6–9] than others [10–13] in predicting the spin-density distribution and other properties of the phenoxyl radical. One of the most common features arising from these calculations is that the experimental ordering of the spin density in the phenoxyl radical is not well reproduced; the calculations have frequently predicted that the spin density at the *ortho*-position(s) is greater than that at the *para*-position, when in fact the experimental spin density at the *para*-position is approximately twice as great as that at the *ortho*-position.[14,15] Such a prediction is not restricted to phenoxyl radicals but has been noted for a number of π-type radicals, including the isoelectronic benzyl and anilino-radicals.[16] The inability of MO methods to reproduce the experimental ordering of the hyperfine splitting constants in radicals has long been a subject of interest, and calculations have suggested [17] that distortion of the molecule must be taken into account in order to reproduce the experimental ordering. In π radicals, spin-density distribution is critically dependent on the geometry of the radical.[16–18] With the geometry of Figure 2a and using the largest reported Gaussian atomic orbital basis set (equivalent to a minimal double-zeta basis set), Hinchliffe [6] obtained the results for the phenoxyl radical shown in Table 1 in a spin-unrestricted MO calculation. The hyperfine constants given are those obtained after a single annihilation on the UHF (unrestricted Hartree–Fock) wave function. Although the correct ordering of the *ortho*- and *para*-proton hyperfine coupling constants is obtained, the absolute values are in poor agreement with experiment, particularly at the *meta*-position. This is reflected in the value of $\langle S^2 \rangle_{AA}$ (total spin eigenvalue after a single annihilation), which deviates substantially from the value of 0.75 expected for a pure doublet state. Although the total energy calculated is the lowest reported for a calculation on the phenoxyl radical, the proton hyperfine coupling constants are not appreciably better than those obtained using cruder basis sets. It is worth noting here that the bond length chosen by Hinchliffe for the C–O bond (1.47 Å) seems inordinately long for a C–O bond which is likely on intuitive grounds to have partial double-bond character (C–O in phenol is 1.36 Å). It has been suggested [6] that a very large

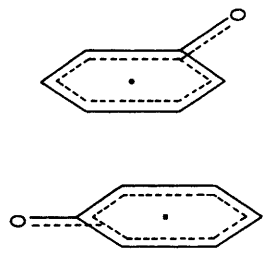

Figure 1. Transition state in the coupling of two phenoxyl radicals

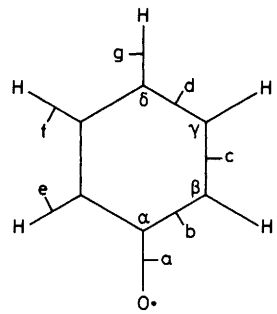

Figure 2. Geometry of the phenoxyl radical

	a Hinchliffe geometry *	b MINDO/3 geometry †	c INDO geometry ‡
α/°	120	115.2	118.0
β/°	120	121.5	119.2
γ/°	120	120.8	121.7
δ/°	120	120.2	120.2
a/Å	1.47	1.216	1.24
b/Å	1.40	1.489	1.50
c/Å	1.40	1.388	1.32
d/Å	1.40	1.425	1.44
e/Å	1.09	1.105	1.07
f/Å	1.09	1.106	1.03
g/Å	1.09	1.104	1.12

* Ref. 6. † Ref. 19. ‡ Ref. 20.

Table 1. Electronic, nuclear, and total energy, and magnetic properties of the phenoxyl radical (experimental data in parentheses from refs. 14 and 15)

	E (hartree)	^{1}H hyperfine coupling constants (G)	$\langle S^2 \rangle$
Nuclear	248.579 63 [a]	a_2 −6.1,[a] −5.62 [b] (−6.60)	$\langle S^2 \rangle_{BA}$ 1.33 [a]
Electronic	−564.029 13 [a]	a_3 8.5,[a] 3.83 [b] (1.96)	
Total	−315.449 50 [a]	a_4 −6.9,[a] −6.08 [b] (−10.40)	$\langle S^2 \rangle_{AA}$ 1.05,[a] 0.825 [b]

[a] Ref. 6. [b] Ref. 19.

basis set needs to be used in order to obtain an UHF wave function which adequately describes the spin properties of such systems. We therefore decided to investigate the effect of basis-set size on the properties of the phenoxyl radical.

Owing to the inherent difficulty in determining the molecular structure of such radicals by experimental methods, most workers have tended to assume a geometry which is based on analogous, stable compounds of known structure. In the case of the phenoxyl radical, most previous workers have assumed a regular hexagonal arrangement for the aromatic ring, with an appropriate C–O bond length. *Ab initio* calculations on the isoelectronic species benzyl, anilino, and phenoxyl radicals have been reported.[6] In all three cases, the geometry chosen was based on the regular hexagon and having appropriate exocyclic C–C, C–N, and C–O bond lengths. This geometry for the phenoxyl radical is shown in Figure 2a. We shall refer to this geometry as the ' Hinchliffe geometry '. It has become clear that the results of the calculation are strongly geometry-dependent (see later discussion) and, hence, we adopted an approach in which different geometries were studied.

It is, of course, possible to obtain an optimum geometry by quantum mechanical methods, *i.e.* by minimising the energy with respect to all the geometrical variables in the molecule. In the case of the phenoxyl radical, the large number of such variables necessarily calls for semi-empirical methods to be used and, indeed, MINDO/3 [19] and INDO [20] optimisations of phenoxyl radicals have been reported.

The geometry obtained by Bischof [19] in the MINDO/3 optimisation is shown in Figure 2b. The major difference between this and the Hinchliffe geometry lies in the shortening of the C(2)–C(3) and the C–O bonds. Bischof's results for the phenoxyl radical using this geometry (henceforth denoted the MINDO/3 geometry) are presented in Table 1. The hyperfine splitting constants were obtained from the spin density matrix using the McConnell relationship,[7] with Q −28 G. Although the absolute values are somewhat underestimated, they do show the correct ordering. In addition, the value of $\langle S^2 \rangle$ is considerably improved over the Hinchliffe case and is much closer to the value expected for a single unpaired electron (0.75). This situation is not uncommon; semi-empirical calculations often afford ' better ' results than the more rigorous *ab initio* calculations due to their parametrisation procedures.

The geometry, obtained by an optimisation under the INDO formalism [20] is shown in Figure 2c. It is clear that the geometry is dependent on the level of approximation at which it is optimised. In this case, the C(2)–C(3) shortening is more marked than in the MINDO/3 case.

Basis Sets and Hamiltonian.—The *ab initio* calculations employed the ATMOL 3 suite of programs [21] and involved the use of a number of different minimal basis sets of varying size and complexity. STO-3G and STO-5G basis sets were constructed using the orbital exponents of Clementi and Raimondi.[22] For the calculations involving contracted Gaussian basis sets, the exponents and coefficients derived by Roos and Siegbahn [23] for first-row elements were employed for the $\langle 7s, 3p \rangle$ case and those of Dunning [24] in the $\langle 9s, 5p \rangle$ calculations. The contraction for the hydrogen 1*s* orbital is that given by Huzinaga.[25] Both restricted and unrestricted Hartree–Fock calculations on the radical were performed. In the latter case, however, a single determinantal wavefunction of the Slater type is not, in general, an eigenfunction of the total spin operator $\hat{S}^2$. This gives rise to the phenomenon of spin contamination, which is partially circumvented in the usual manner [26] by spin annihilation of the major contaminating multiplet.

Results and Discussion

All three geometries were used in the present investigation of the effects of basis-set size and geometry on the properties of the phenoxyl radical. Now, the results of the semi-empirical geometry optimisations suggest that Hinchliffe overestimated the C–O bond length and, hence, an investigation of the effect of varying the C–O distance was also carried out. These calculations were performed using an STO-3G minimal basis set and Tables 2 and 3 give the results of the UHF and RHF calculations, respectively.

The results show that, although one wavefunction gives a better representation than another from the energy point of view (the energy using the MINDO/3 geometry is better than that obtained using the Hinchliffe geometry), it may be quite inferior for the calculation of other properties, *e.g.* the value of $\langle S^2 \rangle_{AA}$ for the two geometries. The value of the total spin operator, $\langle S^2 \rangle$, even after a single annihilation, still shows multiplet contamination of the UHF wave function, expecially in the case of the MINDO/3 geometry. This result is reflected in the poor quality of the proton hyperfine coupling constants calculated for both geometries. In both cases, the value of a_2 is consistently greater than a_4, in contrast with the experimental ordering. The values of a_3 are consistently overestimated, a result in keeping with the calculations of other workers (*cf.* Hinchliffe's results, Table 1). In all cases the spin density on the oxygen (ρ_O) is too large, though this is reduced as the C–O bond length is shortened, *i.e.* the amount of delocalisation of the unpaired electron is increased.

Equivalent RHF STO-3G calculations are shown in Table 3. Spin-restricted SCF calculations give rise to $\langle S^2 \rangle = 0$ in all cases. The total energy obtained in RHF calculations is always higher than the total energy in corresponding UHF calculations, a consequence of using a more rigid basis set in the former. The spin density on the oxygen atom is greatly overestimated, even in those cases where a short C–O bond length is used. Little delocalisation of the unpaired electron is shown, as evidenced also by the extremely low proton hyperfine coupling constants, although the delocalisation does increase as the C–O distance is reduced. The ordering of a_2 and a_4 is, moreover, not in agreement with experiment.

The basis-set size was next increased in a STO-5G minimal basis-set UHF calculation. Table 4 show the results of such a calculation for the MINDO/3 geometry. This increase in basis-set size yields significant improvement in the total energy (*ca.* 3 hartree). It seems surprising, in view of the fact

Table 2. Variation of properties of PhO· with C–O distance in the Hinchliffe and MINDO/3 geometries (UHF STO-3G)

	Hinchliffe geometry			MINDO/3 geometry		Observed
C–O (Å)	1.47	1.40	1.22	1.30	1.22	
$\langle S^2\rangle_{AA}$	1.309	1.304	1.267	1.574	1.444	0.75
a_2 (G)	−7.1	−7.5	−9.0	−9.2	−9.9	−6.6
a_3 (G)	4.3	4.3	4.4	4.7	4.7	1.96
a_4 (G)	−6.72	−7.1	−8.4	−8.9	−9.5	−10.4
ρ_O	0.71	0.67	0.51	0.52	0.43	
E_{tot} (hartree)	−300.968 49	−300.968 09	−300.927 07	−300.977 68	−300.960 49	

Table 3. Variation in total energy of PhO· and spin-density distribution with C–O distance with Hinchliffe and MINDO/3 geometries (RHF STO-3G)

	Hinchliffe geometry		MINDO/3 geometry	
C–O (Å)	1.47	1.22	1.30	1.22
a_2 (G)	−0.57	−2.70	−1.59	−2.88
a_3 (G)	0	0	0	0
a_4 (G)	−0.29	−1.23	−0.95	−1.87
ρ_O	0.95	0.80	0.85	0.72
E_{tot} (hartree)	−300.9462	−300.8841	−300.9283	−300.9017

Table 4. Comparison of STO-3G and STO-5G basis sets

	STO-3G	STO-5G	Hinchliffe	Observed
E_{tot} (hartree)	−300.960 49	−303.754 84	−315.449 50	
$\langle S^2\rangle_{BA}$	1.5807	1.6163	1.3333	0.75
$\langle S^2\rangle_{AA}$	1.4449	1.5167	1.0541	0.75
a_2 (G)	−10.0	−10.0	−6.1	−6.6
a_3 (G)	4.6	4.8	8.5	1.96
a_4 (G)	−9.5	−9.6	−6.9	−10.4

Table 5. UHF and RHF calculations with varying basis sets

	E_{tot}	$\langle S^2\rangle_{BA}$	$\langle S^2\rangle_{AA}$	a_2 (G)	a_3 (G)	a_4 (G)	ρ_O
Single zeta $\langle 7s, 3p\rangle$ calculation							
UHF	−304.021 79	1.509	1.307	−9.8	4.6	−9.52	0.43
RHF	−303.969 11			−3.36	0	−2.24	0.68
Double zeta $\langle 7s, 3p\rangle$ calculation							
UHF	−304.581 23	1.447	1.210	−9.8	4.6	−9.8	0.39
RHF	−304.534 87			−5.6	0	−7.6	0.28
Single zeta $\langle 9s, 5p\rangle$ calculation							
UHF	−304.726 84	1.510	1.310	−9.8	4.6	−9.6	0.43
RHF	−302.663 81			−3.08	0	−2.24	0.67
Double zeta $\langle 9s, 5p\rangle$ calculation							
UHF	−304.885 85	1.454	1.221	−10.1	4.9	−10.2	0.39
RHF	−304.840 01			−5.91	0.1	−7.65	0.25
Double zeta $\langle 9s, 5p\rangle$ calculation on the Hinchliffe geometry							
UHF	−304.584 84	1.401	1.146	−6.98	4.30	−6.68	0.71
RHF	−304.566 41			−0.68	0	−0.3	0.93
Hinchliffe	−306.746 80 (corrected)	1.333	1.054	−6.1	8.5	−6.98	

that the MINDO/3 geometry is of lower energy than the Hinchliffe geometry (see Table 2), that there should be such a discrepancy in total energy between Hinchliffe's calculation and the STO-5G results, even taking Hinchliffe's superior basis set into consideration. This difference can be attributed to an underestimation in the nuclear repulsion energy calculated by Hinchliffe for his own geometry (see Table 1) and the value of 256.2823 hartree calculated on the *same* geometry in our STO-3G calculations. Nuclear repulsion energy depends only on the nuclear co-ordinates and, since these are identical in both cases, there should be no difference in the values of the nuclear repulsion energy calculated. The total energy obtained by Hinchliffe should, therefore, be reduced by 8.7027 hartree. The result is −306.7468 hartree, which is still the lowest value yet calculated for the phenoxyl radical. No improvement in the spin-density distribution was observed on increasing the size of the basis set (Table 4). Indeed, the degree of contamination of the UHF wave function by unwanted multiplets is more severe in the STO-5G case and this suggests that a careful choice of basis set is equally as important as is size of the basis set.

The size of the present basis set was next increased by using contracted gaussian-type bases rather than Slater-type orbitals.

Both single zeta [a total of 132 GTOs contracted into 40 in the $\langle 7s, 3p\rangle$ case and 188 GTOs contracted into 40 in the $\langle 9s, 5p\rangle$ case] and double zeta [a total of 132 GTOs contracted into 80 in the $\langle 7s, 3p\rangle$ case and 188 GTOs contracted into 80

Table 6. Variation in properties of PhO· with C–O distance in the INDO geometry

C–O (Å)	E_{tot} (hartree)	$\langle S^2 \rangle_{AA}$	a_2 (G)	a_3 (G)	a_4 (G)	ρ_O
1.22	−303.977 98	1.1203	−8.20	4.12	−12.32	0.40
1.24	−303.986 50	1.1471	−8.09	4.12	−12.04	0.43
1.26	−303.993 74	1.1756	−7.95	4.12	−11.82	0.45
1.28	−303.999 83	1.1991	−7.84	4.12	−11.48	0.48
1.30	−304.004 88	1.2226	−7.73	4.12	−11.28	0.50
1.32	−304.008 97	1.2435	−7.59	4.12	−11.06	0.52
1.38	−304.015 31	1.2898	−7.31	4.16	−10.64	0.57

Table 7. Phenol radical cation, UHF single-zeta calculations

	C–O (Å)			
	1.24		1.36	
	Orthogonal	Non-orthogonal	Orthogonal	Non-orthogonal
E_{tot} (hartree)	−304.2402	−304.2515	−304.2552	−304.2652
$\langle S^2 \rangle_{AA}$	0.797	0.808	0.804	0.830
a_2 (G)	−6.4	−6.7	−5.9	−6.2
a_3 (G)	2.7	2.8	2.5	2.8
a_4 (G)	−13.4	−13.6	−12.5	−12.3
ρ_O	0.14	0.17	0.19	0.26

in the $\langle 9s, 5p \rangle$ type] calculations were carried out. Table 5 shows the results of the single- and double-zeta contracted gaussian basis-set calculations. Both unrestricted and restricted SCF wavefunctions were obtained. The MINDO/3 geometry was used in all cases. Comparison of the single-zeta results with those obtained from the corresponding STO-3G and STO-5G calculations (Table 4) shows that the gaussian basis gives a better description of the phenoxyl radical than the Slater-type, as the total energy is lowered and the degree of spin contamination is reduced. However, the spin-density distribution is no better, the same trends as before appearing. When the number of degrees of freedom in the wave function is increased by the double-zeta basis, there results a number of improvements with respect to total energy, spin contamination, and proton hyperfine coupling constants. In fact, for the first time, the experimental ordering of a_2 and a_4 is reproduced theoretically from the double-zeta RHF calculation, although the absolute values are somewhat low. We find, then, that doubling the size of the basis set gives better agreement with experiment.

A further increase in the basis-set size to $\langle 9s, 5p \rangle$ does not improve the results relative to those from the $\langle 7s, 3p \rangle$ calculations to any appreciable extent (Table 4).

For comparison, a double-zeta $\langle 9s, 5p \rangle$ calculation consisting of 188 primitive GTOs contracted into 80 GTOs (*cf.* Hinchliffe's 195 primitive GTOs contracted into 80) was performed (Table 5) using the Hinchliffe geometry. These results show that, despite a sophisticated basis set, if the chosen geometry is not a close representation of the true structure, then the agreement of theory with experiment is likely to be poor. For instance, if the spin-density distribution from the last calculation is compared with that of the single-zeta $\langle 7s, 3p \rangle$ calculation, which adopts the MINDO/3 geometry, then the results from the Hinchliffe geometry are no better as far as the hyperfine coupling constants are concerned and considerably worse as regards the spin density on the oxygen atom. A large basis set, however, in conjunction with a more realistic geometry (MINDO/3), gives considerably better results.

A series of single zeta $\langle 7s, 3p \rangle$ UHF calculations on the phenoxyl radical was performed on the INDO geometry,[20] with varying C–O bond lengths. The results are given in Table 6. First, the experimental ordering of the proton hyperfine coupling constants is reproduced at all C–O bond lengths. The absolute values are also in reasonable agreement with experiment. Furthermore, the values of $\langle S^2 \rangle_{AA}$, after a single annihilation, are lower than any others obtained, excepting the double-zeta calculations, probably reflecting the improved spin-density distribution. However, the calculations with the longer C–O bond lengths exhibit a greater degree of spin contamination in the UHF wave function.

The main difference in geometry between the INDO and MINDO/3 optimisations lies in the length of the C(2)–C(3) bond. The shorter this bond becomes (*i.e.* the more double-bond character it possesses), then the greater the delocalisation of the unpaired electron onto the *para*-position. This is shown by comparison of the values of a_4 in the $\langle 7s, 3p \rangle$ SCF calculations on both geometries. Although the INDO geometry predicts the correct ordering of the *ortho*- and *para*-carbon proton hyperfine coupling constants, the values themselves are slightly overestimated. In an attempt to improve the results using the INDO geometry, a calculation in which the length of the C(2)–C(3) bond was increased from 1.32 to 1.34 Å was performed. This had the desired effect of reducing the spin density at the *para*-position but only at the expense of a concomitant and undesirable increase in the spin density at the *ortho*-positions. In addition, a poorer value of $\langle S^2 \rangle$ was obtained.

The value of $\langle S^2 \rangle_{AA}$ is vastly improved if the phenoxyl radical is protonated. Two extremes of conformation can be envisaged for the phenol radical cation, an orthogonal one (O–H out of the plane of the ring) and a non-orthogonal one (O–H in the plane of the ring). The results of a series of single-zeta $\langle 7s, 3p \rangle$ UHF calculations on these geometries are given in Table 7. It has been suggested [27] that there is less double-bond character in the C–O bond of the phenol radical cation than in the phenoxyl radical itself, since the g factor of the phenoxyl radical is similar to that of the radical RĊHCHO, whereas that of the phenol radical cation relates better to RĊHCH$_2$OH. Our calculations bear this suggestion out: the spin-density distribution at the longer C–O bond length is in closer agreement with experiment than that of the shorter C–O bond-length calculation. As above, in the calculations on the phenoxyl radical using the INDO geometry, the proton hyperfine coupling constant at the *para*-position of the phenol radical cation, a_4, is overestimated. However, the

Table 8. Results of double-zeta UHF calculations on INDO geometry

	$\langle 7s, 3p \rangle$	$\langle 9s, 5p \rangle$
E_{tot} (hartree)	−304.572 64	−304.875 33
$\langle S^2 \rangle_{BA}$	3.3414	1.3251
$\langle S^2 \rangle_{AA}$	1.0744	1.0553
a_2 (G)	−8.31	−8.52
a_3 (G)	4.20	4.31
a_4 (G)	−12.27	−11.98
ρ_O	0.395	0.399

values of a_2 and a_3 are much closer to the experimentally observed values than they were in the corresponding calculations on the phenoxyl radical. The spin density at the oxygen atom is also much improved. The improvement in the value of $\langle S^2 \rangle_{AA}$ can be attributed to the removal of those electrons from the π system of the radical which cause the contamination of the wavefunction in the radical [*i.e.* the spin density at the *meta*-positions and C(1)]. These electrons become localised in the new O–H bond and populate the 1*s* orbital of the extra hydrogen atom.

For completeness, UHF double-zeta calculations on the INDO optimisation of the phenoxyl radical were performed, the results of which are given in Table 8.

The total energy of the radical and the value of $\langle S^2 \rangle_{AA}$ are only marginally improved relative to the corresponding single-zeta calculations, as observed in the double-zeta calculations described previously. No improvement in the spin-density distribution is observed at all. There does not seem to be any significant advantage to be gained in employing the larger $\langle 9s, 5p \rangle$ basis set rather than the $\langle 7s, 3p \rangle$ basis set.

We conclude that basis-set size, although important, is not the over-riding factor in determining whether or not the properties of these species are well reproduced. It seems to be far more important to adopt a realistic geometry (*e.g.* MINDO 3 or INDO results), expecially in the case of π radicals, where spin-density distribution has been shown to depend critically on the geometry.

Acknowledgement

One of us (C. C.) thanks the S.E.R.C. for a maintenance grant.

References

1 Part 6, D. R. Armstrong, C. Cameron, D. C. Nonhebel, and P. G. Perkins, preceding paper.
2 I. Fleming, ' Frontier Orbitals and Organic Chemical Reactions,' Wiley, London, 1976, 195.
3 H. Musso, ' Oxidative Coupling of Phenols,' eds. W. I. Taylor and A. R. Battersby, Dekker, New York, 1967, p. 1.
4 R. K. Haynes, H. Hess, and H. Musso, *Chem. Ber.*, 1974, **107**, 3723.
5 Part 8, D. R. Armstrong, C. Cameron, D. C. Nonhebel, and P. G. Perkins, following paper.
6 A. Hinchliffe, *Chem. Phys. Lett.*, 1974, **27**, 454.
7 H. M. McConnell, *J. Chem. Phys.*, 1956, **24**, 764.
8 O. Martensson and G. Karlsson, *Arkiv. Kemi*, 1969, **31**, 5.
9 D. Murphy, *J. Chem. Res.* (*S*), 1980, 321.
10 J. A. Pople, D. L. Beveridge, and P. A. Dobosh, *J. Am. Chem. Soc.*, 1968, **90**, 4201.
11 C. Besev, *Acta Chem. Scand.*, 1963, **17**, 2281.
12 R. W. Fessenden and R. H. Schuler, *J. Chem. Phys.*, 1963, **39**, 2147.
13 R. V. Lloyd and D. E. Wood, *J. Am. Chem. Soc.*, 1974, **96**, 659.
14 T. J. Stone and W. A. Waters, *J. Chem. Soc.*, 1964, 213.
15 W. T. Dixon and R. O. C. Norman, *J. Chem. Soc.*, 1964, 4857.
16 T. Amano, Y. Osamura, E. Kai, and K. Nishimoto, *Bull. Chem. Soc. Jpn.*, 1980, **53**, 2163.
17 H. G. Benson and A. Hudson, *Mol. Phys.*, 1971, **20**, 185.
18 D. L. Beveridge and E. Guth, *J. Chem. Phys.*, 1971, **55**, 458.
19 P. Bischof, *J. Am. Chem. Soc.*, 1976, **98**, 6844.
20 Y. Shinagawa and Y. Shinagawa, *J. Am. Chem. Soc.*, 1978, **100**, 67.
21 V. R. Saunders and M. J. Guest, ' ATMOL 3,' Atlas Computing Division, SRC Rutherford Laboratory, 1976.
22 E. Clementi and D. L. Raimondi, *J. Chem. Phys.*, 1963, **38**, 2686.
23 B. Roos and P. Siegbahn, *Theor. Chim. Acta*, 1970, **17**, 209.
24 T. H. Dunning, jun., *J. Chem. Phys.*, 1970, **53**, 2823.
25 S. Huzinaga, *J. Chem. Phys.*, 1965, **42**, 1297.
26 T. Amos and L. C. Snyder, *J. Chem. Phys.*, 1964, **41**, 1793.
27 W. T. Dixon, *J. Chem. Soc., Faraday Trans. 2*, 1976, 1221.

Received 29*th June* 1982; *Paper* 2/1082